Achievements in Coordination, Bioinorganic and Applied Inorganic Chemistry
Edited by M. Melník, J. Šima, and M. Tatarko
Slovak Technical University Press, Bratislava © 2007

DESIGN, SYNTHESIS AND METAL ION BINDING PROPERTIES OF A PEPTIDE MIMICKING THE ACTIVE CENTRE OF PURPLE ACID PHOSPHATASES

I.N. Jakab[a], Zs. Jenei[a], B. Gyurcsik[a]*, T. Gajda[a], T. Körtvélyesi[b], A. Mikulová, L. Rulíšek[c], T. Raskó[d], and A. Kiss[d]

[a]*Department of Inorganic and Analytical Chemistry, University of Szeged, Dóm tér 7, H-6701 Szeged, P.O. Box 440, Hungary*
[b]*Department of Physical Chemistry, University of Szeged, Rerrich B. tér 1, H-6720 Szeged, Hungary*
[c]*Gilead & IOCB Research Center, Institute of Organic Chemistry and Biochemistry, Academy of Sciences of the Czech Republic, Flemingovo nám. 2, 166 10, Prague 6, Czech Republic*
[d]*Institute of Biochemistry, Biological Research Center of the Hungarian Academy of Sciences, Temesvári krt. 62, H-6726 Szeged, Hungary*
[*]*e-mail: gyurcsik@chem.u-szeged.hu*

ABSTRACT

The aim of our work was to synthesize an oligopeptide molecule, structurally and eventually functionally mimicking the active site of purple acid phosphatase enzymes. Using computational methods we have designed a 20 amino acid containing peptide (P20 = YKDPPTDHLDQRVLDLPHHN) with a stable backbone conformation, capable of forming binding sites for the two natural metal ions of purple acid phosphatases: Zn(II) and Fe(III). The calculations showed that there is a non-zero probability for the metal ions to bind in the folded metal binding sites. The P20 oligopeptide was expressed in E. coli as a Glutathione-S-transferase-based fusion protein. The C-terminal part of this protein - enhancing the expression - is fairly flexible, and therefore it is expected that the fusion will not affect the metal ion binding capacity of the peptide molecule. Synchrotron radiation CD spectroscopy performed in the UV wavelength region showed specific metal ion binding at low ligand to metal ratios, while denaturation of the protein occurred at high metal ion excess.

INTRODUCTION

The design of small model complexes targets both the understanding of the structural and functional properties of the active centre of metalloenzymes and the development of synthetic metalloenzymes. Among these enzymes our interest has been directed toward those cleaving phosphate esters. [1] The relevance of these investigations is well known, e.g. the gene specific (chemo)therapy being one of the most promising applications, i.e., the treatment of diseases involving the production of hazardous proteins. Combined with recognition agents (e.g. a DNA binding protein), artificial hydrolases are useful for the non-

oxidative, sequence specific cleavage of nucleic acids and might become important tools in future biotechnology and medicine.

One of the most thoroughly studied classes of the metallo-phosphoester-hydrolases is the family of purple acid phosphatases (PAPs), which utilize bimetallic active sites (one Fe^{3+} and a second divalent ion, commonly Zn^{2+}, Mn^{2+} or Fe^{2+}) to facilitate phosphoester hydrolysis. PAPs are transition metal-containing glycoproteins with optimal performance under acidic conditions (pH ~ 4.9-6.0). Their common purple colour results from a Tyr-O^- →Fe(III) ligand to metal charge transfer transition (LCMT). [2-4] The structure and the mechanism of PAPs isolated from different plants were investigated profoundly by Krebs and co-workers [5-10]. The studies on kbPAP (kidney bean purple acid phosphatase) and spPAP (sweet potato purple acid phosphatase) enzymes revealed that the active centers of both enzymes were similar, the two metal ions are bridged by a carboxylate oxygen from an aspartate residue and probably by a bridging hydroxide ion. [8] The open coordination sites at both metal ions are probably occupied by water molecules and/or hydroxide ions. [11] Fe(III) is coordinated to a tyrosine, a histidine and an aspartic acid, while Zn(II) to an asparagine and two histidines in addition. [6] A number of nearby polar residues might be important in the hydrolytic mechanism.

According to the consensus minimum mechanism the phosphate ester coordinates to the divalent metal ion and the hydroxide coordinated to the trivalent metal ion, acts as a general base attacking the phosphate ester. [12] This picture greatly demonstrates the synergistic effect of the two metal ions in catalysis.

For this reason our aim was to design peptide molecules that are able to act as structural and functional models of the active site of purple acid phosphatases. Below the procedure of the design, the preparation of the gene of the selected peptide - containing 20 amino acids – and the expression and purification of the Glutathione S-Transferase (GST) fused peptide will be demonstrated. The metal binding properties of the fusion protein were investigated by means of synchrotron radiation CD (SRCD) spectroscopy.

EXPERIMENTAL PART

Expression and purification of the GST-P20 fusion protein

In the construction process of the gene of the 20 amino acid peptide YKDPPTDHLDQRVLDLPHHN (P20) the following primers were used in the PCR (PTC-150 MJ Research) experiment: 5'-gcgaattctacaaggatcctcccaccgatcacctcgatcagcgcgtcctcgatc-3' and 5'-cggcctcgaggttgtgatggggcagatcgaggacgcgctg-3' with the underlined EcoR I and Xho I restriction endonuclease cleaving sites in the N and C-terminal primers, respectively. The

primers anneal to each other through the 16 base regions at their 3'-ends having an estimated melting point of 348 K, and then a KOD-Plus polymerase enzyme filled the rest of the oligonucleotides into a double stranded fragment. This fragment was then cleaved by the appropriate restriction endonucleases and cloned into the appropriate site of an ampicillin-resistant pGEX-6P plasmid vector (Amersham Bioscience). The resulting plasmid encoding P20 fused to the glutathione-S-transferase protein was transformed into *E. coli* BL21 and bacteria were grown in LB/Amp medium at 37°C. The GST-P20 protein expression was induced by adding 1 mM isopropyl-β-thiogalactoside (IPTG, Sigma) to the culture at OD 0.6 – 0.8, and shaking was continued for 3 hours. Cells were sedimented by centrifugation, then resuspended in PBS buffer (1400 mM NaCl, 100 mM Na_2HPO_4, 20 mM KH_2PO_4, pH 7.4) and disrupted by sonication. The debris was removed by centrifugation (13000 rpm, 4°C), and the supernatant was loaded onto a DEAE-cellulose (Whatman) column (gradient: 0 - 1000 mM NaCl, PBS buffer). The protein-containing fractions were loaded onto a Glutathione Sepharose 4B affinity column (Amersham Bioscience). The column was washed with PBS buffer to remove unbound material, then the bound GST-P20 fusion protein was eluted with 10 mM reduced glutathione (Sigma) in PBS buffer. The protein samples were analyzed by sodium dodecyl sulphate - polyacrylamide gel electrophoresis (SDS-PAGE, all chemicals were Sigma products). The GST-P20 containing fractions were pooled, then concentrated by dialysis against a buffer containing 100 mM NaCl, 50%v/v glycerol, 50 mM TRIS-HCl (pH=8.0). Protein concentration was determined by the Bradford (Sigma) assay. [13]

Apparatus

The synchrotron radiation CD (SRCD) spectra were recorded at the SRCD facility at the UV1 beamline, [14] itself part of the ASTRID storage ring at the Institute for Storage Ring Facilities (ISA), University of Aarhus, Aarhus, Denmark. The light passed from the synchrotron (linear polarization) through a CaF_2 window into a CD instrument purged constantly with nitrogen. The polarization was converted into an alternating circularly polarized light. A CaF_2 photoelastic modulator (PEM, model I/CF50, Hinds Instruments, Hillsboro, OR) operating at 50 kHz was used. The signal was detected with a photomultiplier tube (PMT, 9402B, Electron Tubes, Ruislip, U.K.) fitted with a lock-in amplifier. Camphor-sulfonic acid was used to calibrate the instrument. All spectra were recorded in 1-nm steps with a dwell time of 3 s per step, in 0.50 mm bottle type quartz cells (SUPRASIL, Hellma GmbH, Müllheim, Germany), in the wavelength range 185-350 nm. The protein was dissolved in distilled water (final protein concentration of 0.050 mg/cm^3), and the solution pH

was adjusted with HCl and NaOH solutions; the water baseline was subtracted from the raw CD spectra.

RESULTS AND DISCUSSION

Design of the metal binding peptide sequence

Sequence homology searches approved, that the metal ion binding site of the PAPs is well conserved among the enzymes form very different species, starting from the bacteria, through the plant and animal till the human PAPs. [6,15] The coordinating donor groups are in each case the same, i.e. one Tyr, His, and Asp to Fe(III), while one Asn and two His to Zn(II). The metal ions are bridged, by a further Asp side chain from the protein. The same result was obtained on checking the pdb files from the Protein Data Bank (PDB-ID: 1KBP, 3KBP, 4KBP, 1QFC, 1QHW, 1UTE) by a simple Perl Script program selecting the amino acid side-chains close to the metal ions. In all cases the above set of amino acid side-chains was within the selection. It is obvious that the homology of the metal binding residues of the different PAPs implies a predetermined, well defined active centre.

Based on this knowledge we have decided to design an oligopeptide sequence, including the above counted seven amino acids. The principles of the construction of the appropriate sequence were described elsewhere. [16-18] The 20 amino acid long sequence showing enough flexibility besides it is able to preform a structure suitable for two metal ion binding is shown in Fig. 1.

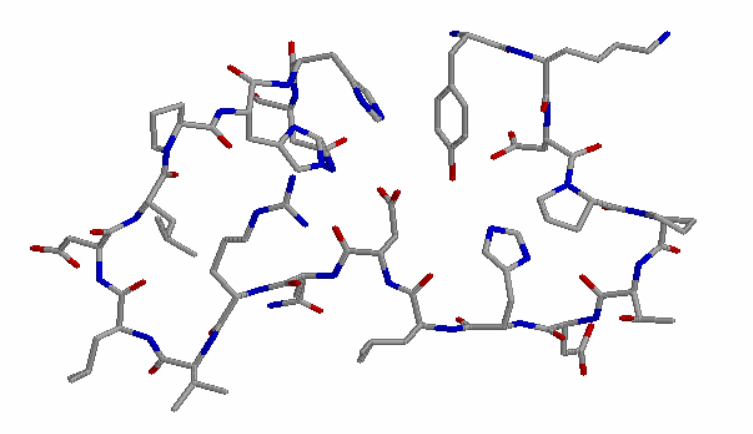

Fig. 1. The proposed structure of the YKDPPTDHLDQRVLDLPHHN (P20) peptide able to preform two adjacent metal ion binding sites with an aspartic acid side-chain between them.

Molecular mechanics calculations with TINKER4.1. [19] as well as GROMACS [20] program packages using the AMBER99 (Assisted Model Building and Energy Refinement) force field [21] were performed to check the intramolecular interactions within the P20 complex molecule in the presence of Fe(III) and Zn(II) ions. To ensure that the proper minimum was reached during the calculation process the system was heated up to 1000 – 1500K for a short time in the equilibration stage, and then let to cool down slowly. This procedure was repeated 2000 times, followed by the geometry optimization. The RMS values on the left part of the Fig. 2 show that the conformation of the peptide has been practically stabilized after ~ 1000 ps of the simulation. On the other hand the higher values of the RMSF on the right part of Fig. 2 indicate, that the two ends of the peptide chain are more flexible than those residues in the middle. These results indicate that the peptide backbone may form a stable template for the binding of the metal ions.

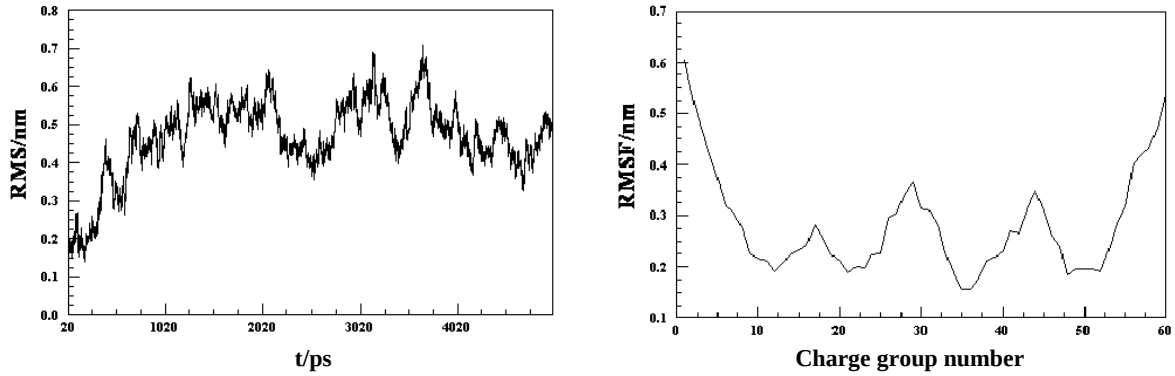

Fig. 2. Left: The change of the RMS values within the 5ns time interval of the simulation. Right: The RMSF (Root Mean Square Fluctuation) values showing the flexibility of the different charge groups within the P20 peptide.

The same feature is reflected in the optimized distances between the different functional groups of the peptide. Clearly, there might be an electrostatic as well as hydrogen bonding interaction between the oppositely charged functional groups of the peptide close in the amino acid sequence e.g. the K(2) and D(3) or D(10) and R(12), respectively remain within 2-8 Å distance from each other. It is also interesting to note, that the Y side-chain forms a close contact (to about 3-4 Å distance) with D(10) reflecting well the structure depicted in Fig. 1.

The metal ions first approached the negatively charged functional groups, i.e. the carboxylate groups of aspartic acids. It seems that the metal ions compete with each other during the time of the simulation for the offered donor groups. The D(7) carboxylate is the only donor group that is approached to less than 5 Å distance by the Zn^{2+}-ion as shown in the left part of Fig. 3. However, on the progress of the time the Fe^{3+}-ion is also becoming

closer to this donor group, while the distance of the Zn^{2+}-ion being slightly increased. As the right part of the figure shows in certain time intervals the D(10) is approached by the both metal ions to almost the same distance. These results do not support the fitting of the metal ions into the preformed binding cavities within the applied conditions, but showed their preference toward the negatively charged donor groups.

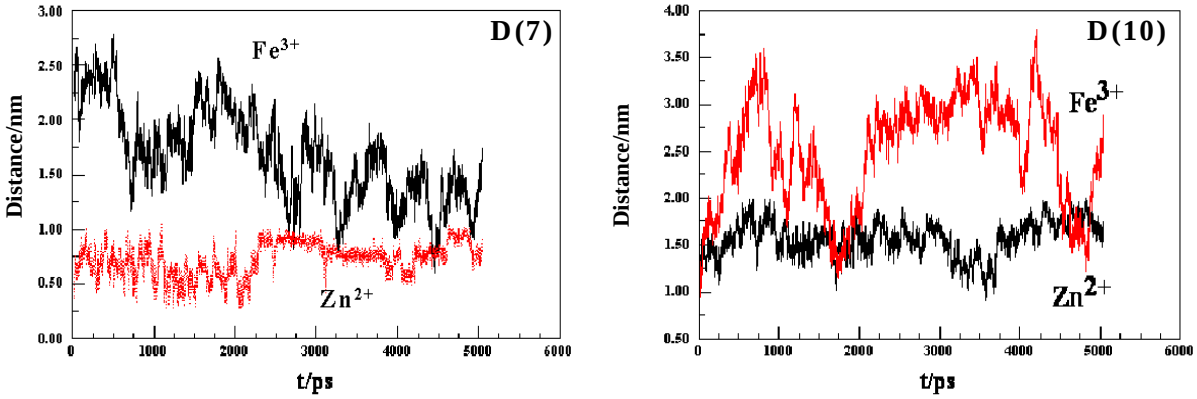

Fig. 3. The change of the distance of the metal ions and D(7) - left - and D(10) - right - side-chain donor groups of P20 peptide within the 5ns of the simulation.

Probably calculations using different solvation models, as well as introducing a hydroxide ion with the ability to bridge the two metal ions may improve the results. Nevertheless, when using an implicit aqueous solvent model in the calculations, both metal ions were removed to about 40-50 Å distance, indicating, that the choice of the solvent model has to be carefully done.

In conclusion the theoretical calculations suggested that the P20 peptide may form a stable backbone conformation, and the charged donor groups might serve as anchoring groups for the metal ions.

Expression and purification of the GST-P20 fusion protein

In order to obtain the P20 peptide we have synthesized the DNA sequence encoding the peptide and cloned this gene into a pGEX-6P plasmid vector as it is described in the experimental part. This vector contains the gene of the glutathione-S-transferase protein (GST), and allows construction of fusions between the C-terminus of GST and the target protein by cloning the gene of the target protein into the vector This type of fusion has several advantages: the fusion protein is expressed at high level, making detection of the product easier, and in most cases allows a one step purification by using a GST-specific affinity column.

Extracts of E. coli cells expressing the GST-P20 fusion protein were analyzed by SDS polyacrylamide gel electrophoresis. In spite of the slight difference in the molecular mass of the two proteins ($M_{r(GST\text{-}P20)}$ = 30512 (261 amino acids), $M_{r(GST)}$ = 28430 (244 amino acids)) the gel (Fig. 4. left panel) clearly shows a small increase of the molecular mass in the case of GST-P20 protein. The level of expression was tested at two different temperatures (307 and 314 K). At the lower temperature, the ratio of the target protein to cell proteins is better for GST, however, it does not affect the GST-P20 expression. It is also important to note, that almost all the expressed target protein was found in the soluble fraction. The right panel of Fig. 4. shows the purity of the GST-P20 preparation obtained by the two-step procedure described in the experimental section.

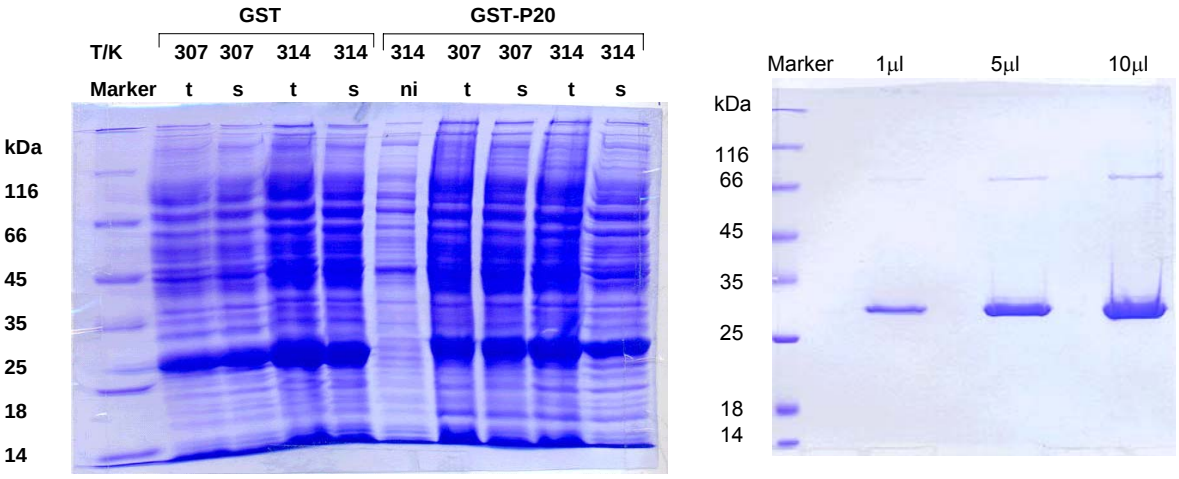

Fig. 4. Left: The SDS-PAGE of extracts of E. coli cells expressing GST-P20. The marks t, s and ni are meant for the total protein content, protein content of the soluble fraction and not induced, respectively. Right: SDS-PAGE of the purified GST-P20 fusion protein.

Running the protein at higher concentrations, a slight band appears at around the double size due to the small extent of dimer formation even under denaturing condition of the gel electrophoresis. The flexibility of the C-terminal part [22] allows the metal ion binding and the hydrolytic activity of the fused peptide in the presence of metal ions. The dimerization [23] is another well known feature of GST that may enhance the above function toward substrates such as the double stranded DNA - taking into account that most of the DNA cleaving nucleases function in their dimeric forms.

SRCD study of the metal ion binding of GST-P20

Synchrotron radiation serves a high flux UV beam, and therefore makes it possible to study the proteins in the UV wavelength interval in low concentrations - using cells with

pathlengths that are too long for the commertial instruments. This is especially important in the case of the proteins expressed in small amounts and in the case of aggregation at higher concentrations. In our case the concentration of the protein was 0.050 mg/cm^3 and it was titrated with Zn(II) solution. As Fig 5. shows at low metal ion:protein ratio there is a slight change in the spectra yielding an isobestic point around 198 nm. This suggests that an equilibrium process occurred between two different species, presumably these are the free protein and its metal complex. With the further increase of the metal ion excess the changes in the spectra are more dramatic, and the new spectra do not cross the isobestic point anymore. The latter process might be attributed to the nonspecific metal ion binding of the bulky protein, and as a consequence a denaturation type changes in the structure. Very similar behaviour was observed while repeating the experiment with Fe(III)ions.

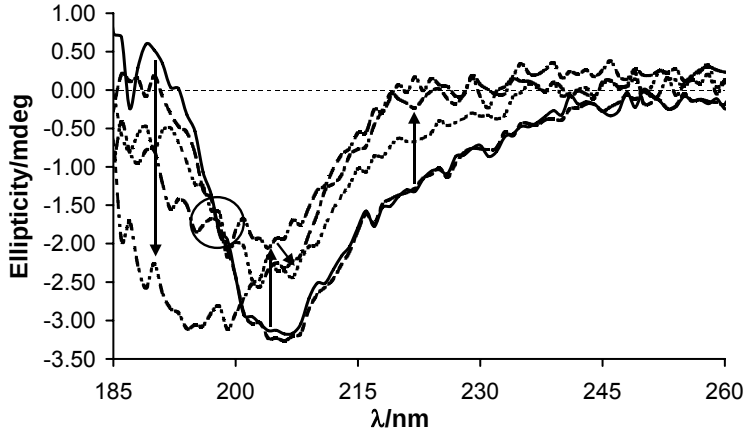

Fig. 5. SRCD spectra of the GST-P20 protein in the absence and presence of increasing Zn(II) concentration. The metal ion to protein molar ratios were: 0:1 (solid line) 2:1, 4:1, 8:1, 16:1 and 32:1. The effect of the changes on increase of metal ion excess are indicated by the arrows, while the circle points out the isobestic point observed at low metal ion excess.

The question arose about the metal ion binding properties of the GST fusion tag itself. The SRCD spectra of GST - as expressed and purified from the pGEX-6P plasmid - were also recorded in the absence and in the presence of increasing amounts of the metal ion. The spectra are shown in Fig. 6.

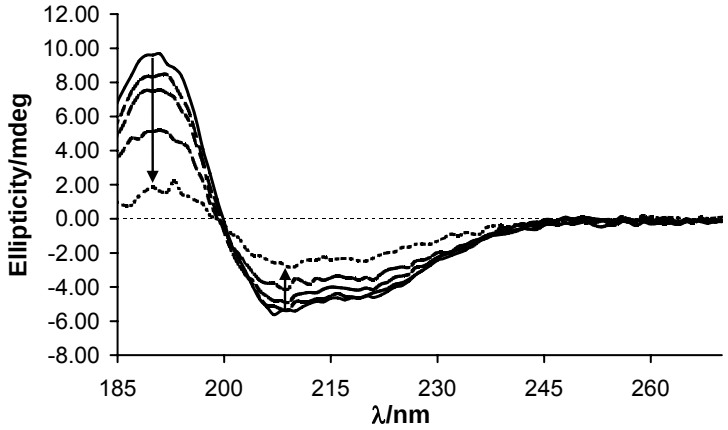

Fig. 6. SRCD spectra of the GST protein in the absence and presence of increasing Zn(II) concentration. The metal ion to protein molar ratios were: 0:1 (solid line) 2:1, 10:1, 21:1and 500:1. The effect of the changes on increase of metal ion excess are indicated by the arrows.

As it can be seen the increase of the metal ion excess here resulted in the continuous decrease of the intensity of the spectra. The spectra cross each other in each case at the zero intensity, which is not considered as an isobestic point. Thus the GST protein undergoes only to a nonspecific metal ion binding and denaturation on increase of the metal ion concentration. The results also indicate, that the structure of the overall protein is affected by the C-terminal fusion of the P20 peptide. However, it has to be noted, that the shape of spectra depend on the expression and purification conditions, while the same pattern of the metal ion binding is observed in each case.

CONCLUSION

In the work presented above we have successfully designed and prepared a metal ion binding oligopeptide P20 in the form of GST-P20 fusion protein. P20 is able to form stable backbone conformation, with cavities for binding of two metal ions. The theoretical calculations showed that the negatively charged functional groups may serve as anchors for metal ion binding. The metal ion binding has been proven by the SRCD experiments on GST-P20. These results showed that at low metal ion to protein ration a specific metal complex is formed, while at higher excess the nonspecific binding dominates causing the denaturation of the protein. The specific metal ion binding was not observed in GST protein itself.

The GST fusion tag represents a number of advantages both in the preparation and purification procedures, and also by allowing the P20 peptide to act independently from the GST. The dimerization ability of GST may enhance the hydrolytic activity of the peptide

complex toward DNA, however, we have to note, that GST is not a target fusion tag in our future investigations.

Instead the genes of the potent short peptides, which possess hydrolytic activity in the presence of metal ions, can be than easily fused using the tools of molecular biology to the genes of specific proteins binding the hydrolytic target molecules. Followed by the expression of these artificial hydrolases, the resulting substrate specificity will be determined by the nature of the fused protein, with a metal binding peptide as the active site. The above idea is supported by a number of investigations on nucleases enlightening that different domains of the protein are responsible for the hydrolytic function and for the substrate specificity. Our future work is directed toward the investigation of the catalytic activity of the P20 peptide.

Acknowledgements

Financial support was provided by the Hungarian National Science Foundation (OTKA NI 12345, K 63606 and K 61577), the European Union Research Infrastructure Action FP6 (Integrated Activity on Synchrotron and Free Electron Laser Science, Contract RII3-CT-2004-506008) and project LC512 of MSMT CR. The authors thank to Prof. Kyosuke Nagata (University of Tsukuba, Japan) for his helpful suggestions on the constraction of plasmid.

REFERENCES

1 B.N. Trawick, A.T. Daniher, J.K. Bashkin, Chem. Rev., 1998, 98, 939-960
2. J.B. Vincent, G.L. Olivier-Lilley, B.A. Averill, Chem. Rev., 1990, 90, 1447-1467
3. D.E. Wilcox, Chem. Rev., 1996, 96, 2435-2458
4. D. Gani, J. Wilkie, Struct. Bonding, 1997, 89, 133-175
5. W.N. Lipscomb, N. Strater, Chem. Rev., 1996, 96, 2375-2433
6. T. Klabunde, B. Krebs, Struct. Bonding, 1997, 89, 177-198
7. A. Durmus, C. Eicken, B.H. Sift, A. Kratel, R. Kappl, J. Hüttermann, B. Krebs, Eur. J. Biochem., 1999, 260, 709-716
8. N. Strater, T. Klabunde, P. Tucker, H. Witzel, B. Krebs, Science, 1995, 268, 1489-1492
9. B.H. Sift, A. Durmus, W. Meyer-Klaucke, B. Krebs, J. Synchrotron Rad., 1999, 6, 421-422
10. S. Priggemeyer, P. Eggers-Borkenstein, F. Ahlers, G. Henkel, M. Körner, H. Witzel, H.-F. Nolting, C. Hermes, B. Krebs, Inorg. Chem., 1995, 34, 1445-1454
11. E.L. Hegg, J.N. Burstyn, Coord. Chem. Rev., 1998, 173, 133-165

12. M. Merkx, B.A. Averill, J. Am. Chem. Soc., 1999, 121, 6683-6689
13. M.M. Bradford, Anal. Biochem., 1976, 72, 248-254
14. P. Limao-Vieira, A. Giuliani, J. Delwiche, R. Parafita, R. Mota, D. Duflot, J.P. Flament, E. Drage, P. Cahillane, N.J. Mason, S.V. Hoffmann, M.J. Hubin-Franskin, Chem. Phys. 2006, 324, 339-349
15. T. Klabunde, N. Strater, B. Krebs, H. Witzel, FEBS Lett., 1995, 367, 56-60
16. L. Rulíšek, Z. Havlas, J. Am. Chem. Soc., 2000, 122, 10428-10439
17. L. Rulíšek, Z. Havlas, J. Phys. Chem. A, 2002, 106, 3855-3866
18. L. Rulíšek, Z. Havlas, J. Phys. Chem. B, 2003, 107, 2376-2385
19. J.W. Ponder, TINKER41 (Software Tools for Molecular Design) Version 3.9 (2001)
20. D. van der Spoel, A.R. Van Buuren, E. Apol, J.P. Meulenhoff, D. P. Tieleman, A.L.T.M. Sijbers, R. van Drunen, H.J.C. Berendsen, GROMACS User Manual, University of Gröningen, (1996).
21. S.J. Weiner, P.A. Kollman, D.T. Nguyen, J. Comp. Chem., 1986, 7, 230
22. D.R. Smyth, M.K. Mrozkiewicz, W.J. Mcgrath, P. Listwan, B. Kobe, Protein Sci., 2003, 12, 1313-1322
23. Y. Maru, D.E. Afar, O.N. Witte, M. Shibuya, J. Biol. Chem., 1996, 271, 15353-15357